International Journal of Scientific Research & Engineering Trends
Volume 5, Issue 2, Mar- Apr-2019, ISSN (Online): 2395-566X

Analysis of the Impact of Clear Air Atmospheric Conditions on Propagation Loss at Microwave Frequencies

Ezeh, Ikechukwu H.
Department of Electrical Electronic Engineering
Imo State University (IMSU) Owerri
Imo State Nigeria
ikechukwu4per@yahoo.com

Onwuzuruike, V. Kelechi
Department of Electrical Electronic Engineering
Imo State University (IMSU) Owerri
Imo State Nigeria

***Abstract*- In the paper, the analysis of the impact of clear –air atmospheric conditions on propagation loss at microwave frequencies is presented. Particularly, the study focused on the impact of variation in point refractivity gradient on multipath fade depth based on the International Telecommunication Union (ITU) recommendation P.530-17 quick planning applications method. The point refractivity gradient depends on the vertical profile of the primary radio climatic parameters, namely, atmo spheric temperature, pressure and relative humidity. Accordingly, the Nigerian Meteorological Agency (NIMET) Radiosonde dataset of the atmospheric temperature, pressure and relative humidity for 2014 in Cross River state were used in the study. The twelve months (2014) Radio sonde dataset of the atmospheric temperature, pressure and relative humidity at the ground level and at height of 65 m above ground were used to compute the refractivity (N) and point refractivity gradient (dN1) for each of the 12 months along with the annual average values of N and dN1. The results show that the ITU annual average value of dN1= –400 is over 200 % of the annual average value of -131.86 obtained from the locally measured data. For each of the 12 months multipath fade depth is computed using the point refractivity gradient obtained in the study along with parameters of a 10 km case study microwave link. The results show that at the frequency of 8 GHz and percentage of time Pw (%) of 0.01 % that a given fade depth is exceeded in the average worst month, the maximum fade depth of 18.95865 dB occurred in October whereas the lowest fade depth of 14.10459 dB occurred in April. Also, the multipath fade depth is inversely proportional to the point refractivity gradient. Furthermore, the result for the multipath fade depth at Pw = 0.01 % and frequencies of 8 GHz , 16 GHz and 28 GHz for the 12 months shows that multipath increase with frequency and the ITU dN1 value continues to maintain the highest multipath fade depth in each of the frequencies considered. Also, the result for the multipath fade depth at the frequency of 16 GHz and Pw of 0.001 %, 0.01 % and 0.1 % for the 12 months shows that multipath decrease with Pw and the ITU dN1 value continues to maintain the highest multipath fade depth in each of the Pw values considered. The ideas presented in this paper is relevant to microwave communication link designers as it enables them to determine the appropriate fade margin that can be specified to accommodate the multipath fade depth that can occur in a given link.**

Keywords **–Multipath, Refractivity, Refractivity Gradient, Fading, Microwave Communication, Line of Sight Communication.**

I. INTRODUCTION

In wireless communication systems signals originate from the transmitter and then propagate through the atmosphere to the receiver [1,2,3,4]. As the signal propagates through the atmosphere it is subjected to diverse adverse effects due to the atmospheric conditions. Particularly, the variations in the vertical profile of primary radio climatic parameters, namely, temperature, pressure and relative humidity cause vertical variation in the atmospheric refractivity which in turn causes bending of the signal path [5,6,7,8,9,10,11]. Generally, at microwave frequency signals are known to travel in a straight line. However, due to the vertical profile of the atmospheric refractivity microwave signals are adversely affected resulting in multipath fading, among other effects [12, 13,14,15,16,17,18].Over the years the International Telecommunication Union (ITU) has developed models to determine the multipath fade depth the signals are subjected to clear air atmospheric conditions [19]. The model has undergone several reviews and the latest version is the ITU-R P. 530-17 model [19]. In this paper, the effect of clear air atmospheric conditions on the multipath propagation loss that microwave signals are subjected to in a given case study area based on the

© 2019 IJSRET

ITU-R P. 530-17 model is presented. The study is based on locally measure vertical profile data of the temperature, pressure and relative humidity in the study area. Missing requisite data points are determined using Inverse Distance Weighting (IDW) spatial interpolation technique [20,21]. Monthly and annual average multipath propagation losses are obtained and compared with the ITU values for the given case study area.

II. THE MATHEMATICS OF MULTIPATH FADING

In the latest ITU-R P.530-17 [1] quick planning applications method the percentage of time Pw (%) that fade depth A (dB) is exceeded in the average worst month is given as [19]:

$$Pw = K(d^{3.1})\left(1+|\varepsilon_p|\right)^{-1.29}(f^{0.8})\left(10^{(-0.00089\,h_L - A/10)}\right) \quad (1)$$

Where h_e is height of transmitter antenna and h_r is height of receiver antenna, h_L is the lower antenna height which is the minimum of the two antenna heights; h_e and h_r, the Geoclimatic Factor is K, f is frequency (GHz) and $|\varepsilon_p|$ (in mrad) the path inclination where [19]:

$$|\varepsilon_p| = \left|\frac{h_r - h_e}{d}\right| \quad (2)$$

Where d is the path length (km). The multipath fade depth, $A\ (dB)$ for the given percentage of time Pw (%) s determined as follows;

$$A\ (dB) = -10\left(0.00089h_L - \log\left(\frac{P_w}{\left(K(d^{3.1})(1+|\varepsilon_p|)^{-1.29}\right)(f^{0.8})}\right)\right) \quad (3)$$

Where the geoclimatic factor, K in the latest ITU-R P.530-17 [1] quick planning applications method is given as [19];

$$K = \left(10^{(-4.6\ -0.0027\,dN_1)}\right) \quad (4)$$

Where the point refractivity gradient denoted as dN_1 is the refractivity gradient from ground level to a height of 65 m of the atmosphere. Generally, point refractivity gradient, dN_1 is expressed as the gradient of refractivity from the surface level to a height of 65 m above the ground, that is [16];

$$dN_1 = \frac{N_2 - N_1}{h_2 - h_1} = \frac{N_{(at\ 65m\ height\ from\ ground\ )} - N_{(at\ 0\ m\ height\ from\ ground\ )}}{65} \quad (5)$$

Were h_2 is the height of 65 m above the ground (that means $h_2 = 65\ m$) and h_1 is the at the ground level (that means $h_1 = 0\ m$)

- N_2 is radio refractivity at the height of 65 m above the ground and N_1 is radio refractivity at the surface where the height is zero (m).

Now the radio refractivity, N is given as [16];

$$N = 77.6\left(\frac{P}{T} + 4810\left(\frac{e}{T^2}\right)\right) \quad (6)$$

where T is the absolute temperature in Kelvin; p is the atmospheric pressure in hPa and e is the water vapour pressure The water vapour pressure is given as [16];

$$e = 6.112\left(\frac{H}{100}\right)\ \exp\left(\frac{17.5(t)}{t + 240.97}\right) \quad (7)$$

Where H is the relative humidity in % and t is the atmospheric temperature (Celsius)

III. THE CASE STUDY AREA AND DATA DESCRIPTION

The study is based on vertical profile data of the radio climatic parameters collected by Nigerian Meteorological Agency (NIMET) for cross River state for the year 2014. The data was collected using Radio sonde equipment launched into the atmosphere on selected days in every month of the year. The radio climatic parameters used in the study are the atmospheric temperature, pressure and relative humidity. Particularly, the data on atmospheric temperature, pressure and relative humidity at the ground level and at 65 m above the ground were extracted from the Radio sonde vertical profile data of the case study area for the year 2013.

Usually, the Radio stoned equipment does not give measured data at any specified height but rather the data are captured with respect to time. Consequently, the Inverse Distance Weighting (IDW) spatial interpolation method was used for interpolation of the Radio sonde data to obtain the missing data at the required height 65m. The IDW method is given as [16, 20,21];

$$\acute{Z}(65) = \sum_{i=1}^{i=n}\{(\lambda_i)Z(x_i)\} \quad (8)$$

Where $\acute{Z}$ is the approximated value at the point of interest65 m,

Z is the known value at the sampled point x_i,

n denotes the number of sampled points used for approximation.

λ_i is the weighting parameter and it is given as [16, 20,21];

$$\boldsymbol{\lambda_i} = \frac{\frac{1}{(d_i)^p}}{\sum_{i=0}^{i=n}\left(\frac{1}{(d_i)^p}\right)} \quad (9)$$

Where d_i is the distance between x_0 and x_i, p is a power parameter and n is as denoted previously. The 2014 Radio sonde dataset for the atmospheric temperature, pressure and relative humidity at the ground level, h = 0 and at 65 m above ground is given in Table 1. In Table 1, the values at 65 m are obtained by spatial interpolation of equation 8.

The graph plot for the atmospheric temperature, pressure and relative humidity at the ground level, h = 0 and at 65 m above ground along with their annual average values are given in Figure 1, figure 2 and Figure 3 respectively.

© 2019 IJSRET

International Journal of Scientific Research & Engineering Trends
Volume 5, Issue 2, Mar- Apr-2019, ISSN (Online): 2395-566X

Table 1 The 2014 River state Radio sonde dataset for the atmospheric temperature, pressure and relative humidity at the ground level, h = 0 and at 65 m above ground

Month	T[C]	U %	P[hPa]	T[C]	U[%]	P[hPa]
Jan	32	66	1013.1	29.9	67.2	1005.8
Feb	30.2	67	1013.5	28.3	65.9	1005.5
Mar	24.8	96	1014.2	24.7	91.7	1006.7
April	29.8	70	1013.3	31.1	66.5	1006.0
May	29.5	72	1013	28.4	68.7	1005.6
June	29	77	1014.3	27.8	74.7	1006.9
July	27.5	91	1017.4	26	90.7	1009.9
Aug	26.9	80 .2	1018.3	26.0	80.1	1011.0
Sept	25.9	85	1017.6	25.1	86.7	1010.1
Oct	29.5	75	1016.1	26.3	78.8	1008.6
Nov	28.3	76	1013.6	27.6	77.5	1006.1
Dec	31.8	68	1013.3	30.2 2	67.4	1006.0
Annual Avg.	28.7	76 .9	1014.8	27.6	76.3	1007.3

Source: Nigerian Meteorological Agency (NIMET).

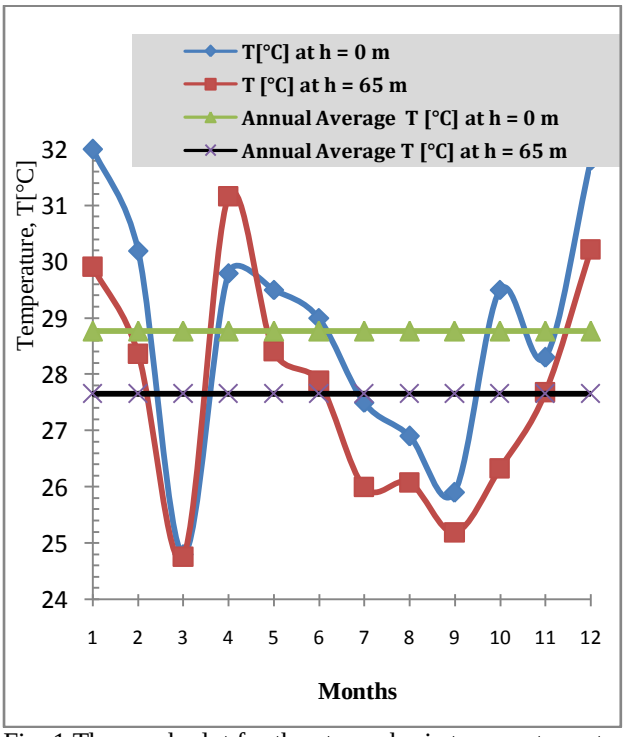

Fig. 1 The graph plot for the atmospheric temperature at the ground level, h = 0 and at 65 m above ground along with their annual average values.

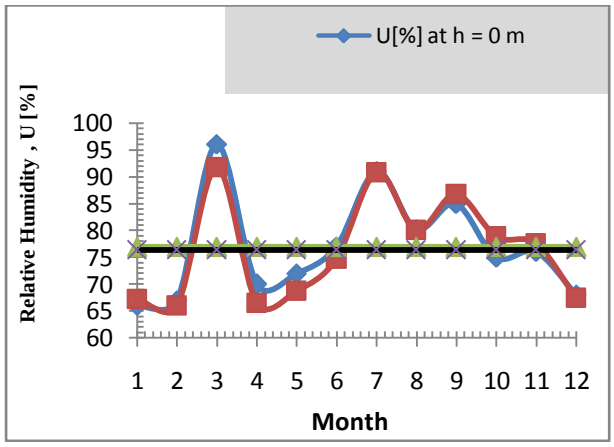

Fig. 2 The graph plot for the relative humidity at the ground level, h = 0 and at 65 m above ground along with their annual average values.

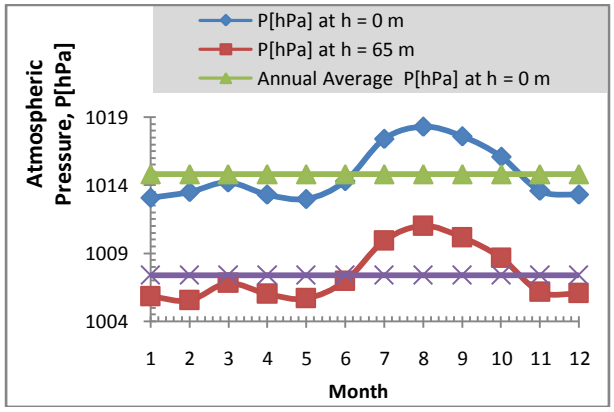

Fig. 3 The graph plot for the atmospheric pressure at the ground level, h = 0 and at 65 m above ground along with their annual average values.

IV. RESULT AND DISCUSSIONS

Based on the radio climatic data in Table 1, the refractivity (N) and point refractivity gradient (dN1) were computed for the 12 months along with the annual average values of N and dN1. The result of the refractivity at the ground level and at the height of 65 m above ground for the 12 months in 2014 is given in Table 2 and Figure 4 and Figure 5. The results show that, for the 12 months refractivity, the values of N at the height of 65 m are lower than their corresponding values at the ground level. Essentially, refractivity decreases with height. The graph plot for the point refractivity gradient (dN1) for the 12 months along with the annual average value is given in Figure 5. The lowest point refractivity gradient value of -193.9[N-Unit/Km] in occurred in October whereas highest point refractivity gradient value of -14.1[N-Unit/Km] in occurred in April.

© 2019 IJSRET

International Journal of Scientific Research & Engineering Trends
Volume 5, Issue 2, Mar- Apr-2019, ISSN (Online): 2395-566X

Table 2 Refractivity at the ground level and at the height of 65 m above ground for the 12 months in 2014.

Month	Height , h = 0 m					Height , h = 65 m					
	T [°C]	U %	P [hPa]	Water vapor pressure , e	N [N-Unit]	T [°C]	U [%]	P [h,Pa]	Water vapor pressure , e	N [N-Unit]	dN1 [N-
Jan	32	66	1013.1	31.1	382.5	30	67	1005.8	28.1	372.0	
Feb	30	67	1013.5	28.5	375.1	28	66	1005.5	25.2	362.6	-191.6
March	25	96	1014.2	29.8	389.5	25	92	1006.8	28.4	381.8	118.6
April	30	70	1013.3	29.1	378.1	31	67	1006.0	29.9	377.2	
May	30	72	1013.0	29.4	379.8	28	69	1005.7	26.4	367.3	
June	29	77	1014.3	30.5	385.7	28	75	1007.0	27.8	374.2	
July	28	91	1017.4	33.1	399.5	26	91	1009.9	30.2	388.3	
August	27	80	1018.3	28.2	380.3	26	80	1011.0	26.8	374.2	
Sept	26	85	1017.6	28.1	381.7	25	87	1010.2	27.5	378.4	
Oct	30	75	1016.1	30.6	385.6	26	79	1008.6	26.8	373.0	
Nov	28	76	1013.6	29.0	380.1	28	78	1006.2	28.5	377.4	
Dec	32	68	1013.3	31.7	385.2	30	67	1006.1	28.7	373.9	
Annual Avg.	29	77	1014.8	29.9	383.6	28	76	1007.4	27.9	375.0	

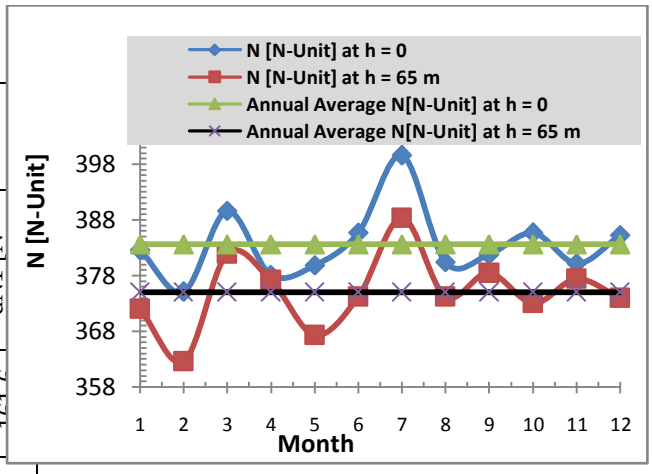

Fig.4 The graph plot for the refractivity at the ground level, h = 0 and at 65 m above ground along with their annual average values.

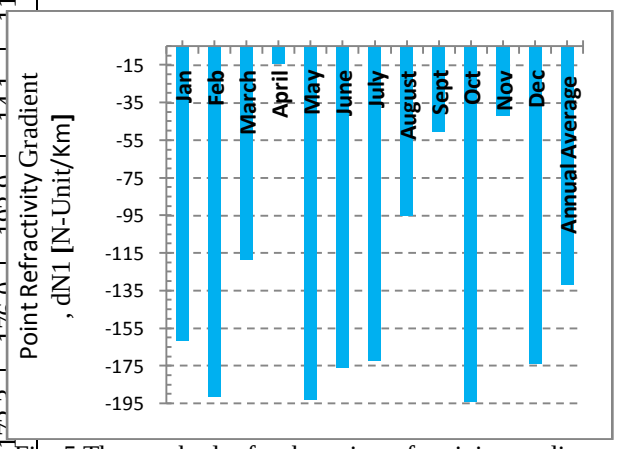

Fig. 5 The graph plot for the point refractivity gradient for the 12 months along with the annual average value.

In addition, for each of the 12 months the multipath fade depth A (dB) is computed using the point refractivity gradient obtained in the study along with microwave link parameters shown in Table 3. Particularly, the computations were conducted for the C-band 8 GHz, the Ku-Band 18 GHz and the Ka-Band 28 GHz. The value of 0.01 % is used for the percentage of time Pw (%) that fade depth A (dB) is exceeded in the average worst month. The result for the point refractivity gradient, multipath fade depth and geoclimatic factor Pw = 0.01 % and frequency = 8 GHz for the 12 months along with the annual average value.

Also shown in Table 4 and Figure 5 is the ITU value for dN1 for the case study site along with the multipath fade depth computed with it. The ITU annual average value for dN1 is over 200 % of the annual average value of -131.86 obtained from the locally measured data. Again, the results showed that the multipath fade depth is

© 2019 IJSRET

inversely proportional to the point refractivity gradient. Also, the maximum fade depth of 18.95865 dB occurred in October whereas the lowest fade depth of 14.10459 dB occurred in April.

Table 3 The microwave link parameters values used to determine the multipath fade depth.

Parameter Name and Unit	Values
Path length, d (km)	10
Antenna heightfor the transmitter, he (m)	115
Antenna height for the receiver, hr (m)	92
Path inclination , ε_p (mrad)	2.3
Point refractivity gradient , dN1	Values computed from the site data and ITU annual average value
Percentage of time Pw (%) that fade depth A (dB) is exceeded in the average worst month	0.001 %, 0.01 % and 0.1 %
Microwave Frequency (GHz)	C-Band 8 GHz
	Ku-Band 16 GHz
	Ka-Band 28 GHz

Table 4 The point refractivity gradient, multipath fade depth and geoclimatic factor Pw = 0.01 % and frequency = 8 GHz for the 12 months along with the annual average value.

Month	dN1	Multipath Fade Depth , A [dB]	Geoclimatic Factor, K
Jan	161.56	18.09	6.86E-05
Feb	-191.6	18.90	8.27E-05
March	-118.59	16.93	5.25E-05
April	-14.1	14.10	2.74E-05
May	-192.86	18.93	8.33E-05
June	-176.01	18.48	7.50E-05
July	-172.26	18.37	7.33E-05
August	-94.91	16.29	4.53E-05
Sept	-50.48	15.09	3.44E-05
Oct	-193.88	18.96	8.38E-05
Nov	-42.06	14.86	3.26E-05
Dec	-173.96	18.42	7.41E-05
Annual Avg. dN1	-131.86	17.28	5.70E-05
ITU Annual Value dN1	-400	24.52	3.02E-04

The result for the multipath fade depth at Pw = 0.01 % and frequency = 8 GHz , 16 GHz and 28 GHz for the 12 months along with the annual average values are shown in Figure 7. The results show that multipath increase with frequency. The ITU value continues to maintain the highest multipath fade depth in each of the frequencies considered. The result for the multipath fade depth at the frequency of 16 GHz and Pw of 0.001 %, 0.01 % and 0.1 % for the 12 months along with the annual average values are shown in Figure 8. The results show that multipath decrease with Pw. Again, the ITU dN1 value continues to maintain the highest multipath fade depth in each of the Pw values considered.

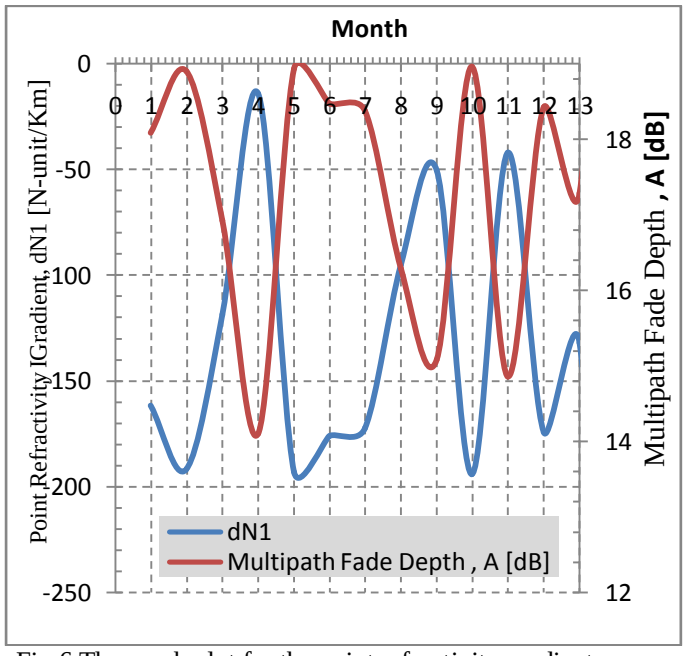

Fig.6 The graph plot for the point refractivity gradient for the 12 months along with the annual average value.

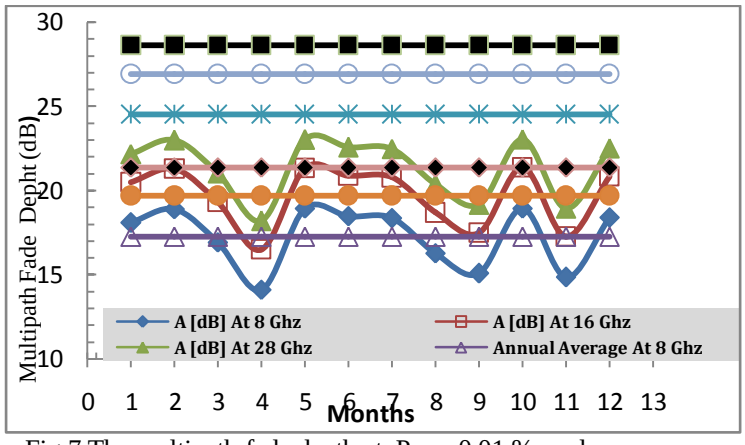

Fig.7 The multipath fade depth at Pw = 0.01 % and frequency = 8 GHz , 16 GHz and 28 GHz for the 12 months along with the annual average value.

© 2019 IJSRET

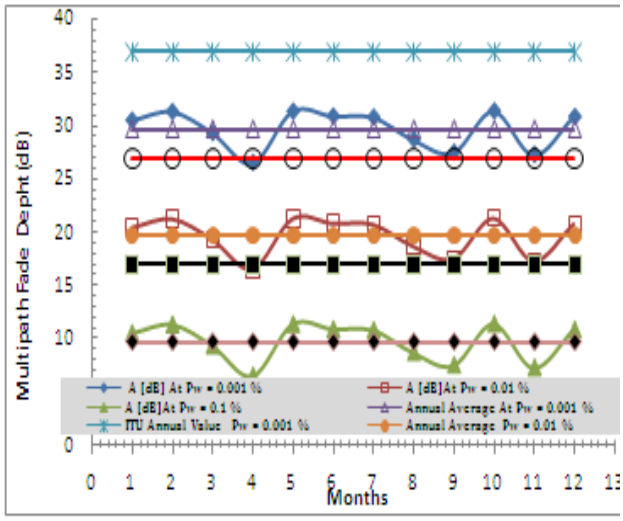

Fig. 8 The multipath fade depth frequency of 16 GHz and Pw = 0.001 % , Pw = 0.01 % and Pw = 0.1 % for the 12 months along with the annual average value.

V. CONCLUSION

Relevant mathematical expressions that are required to compute refractivity and point refractivity gradient from the vertical profile data of primary radio climatic parameters are presented. The primary radio climatic parameters used are atmospheric temperature, pressure and relative humidity. Furthermore, multipath fade depth is computed based on the point refractivity gradient. The aim is to analyze the impact of variation in the atmospheric conditions on the propagation loss, particularly multipath fade depth at the microwave frequency. In this case, the computations were performed for some selected microwave frequencies and expected network outage percentages. The computations were based on a locally measured vertical profile data of atmospheric temperature, pressure and relative humidity. The results obtained were compared with the result of ITU specified value of point refractivity gradient for the case study site. The results show that the ITU annual average value of point refractivity gradient is over 200 % of the annual average value of data obtained from the locally measured data. Also, the multipath fade depth is inversely proportional to the point refractivity gradient. The ideas presented in this paper is relevant to microwave communication link designers as it enables them to determine the appropriate fade margin that can be specified to accommodate the multipath fade depth that can occur in a given link.

REFERENCES

1. Thomas, G. S., & Chandran, C. S. (2018, August). A Review on Autonomous Relay For Millimeter Wave Wireless Communications. In IOP Conference Series: Materials Science and Engineering (Vol. 396, No. 1, p. 012043). IOP Publishing.
2. Pupala, R. N. (2005). Introduction to wireless electromagnetic channels & large scale fading. Department of Electrical Engineering, Rutgers University, Lecture notes for Wireless Communication Technologies course offered by Dr. N. Madhaban, Spring.
3. Zeng, Y., Clerckx, B., & Zhang, R. (2017). Communications and signals design for wireless power transmission. IEEE Transactions on Communications, 65(5), 2264-2290.
4. Bushuev, D., &Arnon, S. (2006). Analysis of the performance of a wireless optical multi-input to multi-output communication system. JOSA A, 23(7), 1722-1730.
5. Bruin, E. R. (2016). On propagation effects in Maritime Situation Awareness: Modelling the impact of North Sea weather conditions on the performance of AIS and coastal radar systems (Master's thesis).
6. Adedayo, K. D. (2016). Statistical analysis of the effects of relative humidity and temperature on radio refractivity over Nigeria using satellite data. African Journal of Environmental Science and Technology, 10(7), 221-229.
7. FALODUN, S. (2015). Quantitative Studies of Vertical Structure of Radio Refractive Index in a Coastal Area of Nigeria. Journal of Sustainable Technology, 6(2).
8. Lentini, N. E., & Hackett, E. E. (2015). Global sensitivity of parabolic equation radar wave propagation simulation to sea state and atmospheric refractivity structure. Radio Science, 50(10), 1027-1049.
9. Mufti, N. (2012). Investigation into the Effects of the Troposphere on VHF and UHF Radio Propagation and Interference between Co-Frequency Fixed Links (Doctoral dissertation, University of Leicester).
10. Mason, S. P. (2010). Atmospheric effects on radio frequency (RF) wave propagation in a humid, near-surface environment. Naval Postgraduate School Monterey Ca.
11. Nievinski, F. G. (2009). Ray-tracing Options to Mitigate the Neutral Atmosphere Delay in GPS (Doctoral dissertation, University of New Brunswick, Department of Geodesy and Geomatics Engineering).
12. AbouAlmal, A., Abd-Alhameed, R. A., Jones, S. M., & Al-Ahmad, H. (2015). New methodology for predicting vertical atmospheric profile and propagation parameters in subtropical arabian gulf region. IEEE Transactions on Antennas and Propagation, 63(9), 4057-4068.
13. Ugwu, E. B. I., Umeh, M. C., &Ugonabo, O. J. (2015). Microwave propagation attenuation due to earths atmosphere at very high frequency (VHF) and

ultra-high frequency (UHF) bands in Nsukka under a clear air condition. International Journal of Physical Sciences, 10(11), 359-363.
14. Bettouche, Y., Agba, B. L., &Kouki, A. B. (2014, August). Geoclimatic factor and point refractivity evaluation in Quebec-Canada. In General Assembly and Scientific Symposium (URSI GASS), 2014 XXXIth URSI (pp. 1-4). IEEE.
15. Asiyo, M. O., &Afullo, T. J. O. (2013). Statistical estimation of fade depth and outage probability due to multipath propagation in Southern Africa. Progress In Electromagnetics Research, 46, 251-274.
16. Asiyo, M. O. (2013). Characterization and Modelling of Effects of Clear Air on Multipath Fading in Terrestrial Links (Doctoral dissertation, University of KwaZulu-Natal, Durban).
17. Kizer, G. (2013). Digital microwave communication: engineering point-to-point microwave systems. John Wiley & Sons.
18. Abu-Almal, A., & Al-Ansari, K. (2010). Calculation of effective earth radius and point refractivity gradient in UAE. International Journal of Antennas and Propagation, 2010.
19. ITU-R P. 530-17 (2017) ITU-R Recommendation P. 530-17, Propagation data and prediction methods required for the design of terrestrial line-of-sight systems," ITU, Geneva, Switzerland . Available at https://www.itu.int/dms_pubrec/itu-r/rec/p/R-REC-P.530-17-201712-I!!PDF-E.pdf. Accessed on November 12, 2018.
20. Tunçay, T., Bayramin, I., AtALAY, F., &Ünver, İ. (2016). Assessment of inverse distance weighting (IDW) interpolation on spatial variability of selected soil properties in the Cukurova Plain. TarımBilimleri Dergisi, 22(3), 377-384.
21. Nusret, D., & Dug, S. (2012). Applying the inverse distance weighting and kriging methods of the spatial interpolation on the mapping the annual precipitation in Bosnia and Herzegovina.

© 2019 IJSRET